catalysts

MDPI

Article

Use of Co/Fe-Mixed Oxides as Heterogeneous Catalysts in Obtaining Biodiesel

Norma Gutiérrez-Ortega [1,*], Esthela Ramos-Ramírez [2,*], Alma Serafín-Muñoz [1], Adrián Zamorategui-Molina [1] and Jesús Monjaraz-Vallejo [2]

[1] Environmental Engineering Laboratory, Department of Civil Engineering, Engineering Division, University of Guanajuato, 36000 Guanajuato, México; sermuah@ugto.mx (A.S.-M.); zamorategui@ugto.mx (A.Z.-M.)

[2] Advanced Materials and Processes Laboratory, Department of Chemistry, Division of Natural and Exact Sciences, University of Guanajuato, 36000 Guanajuato, México; jdj.monjarazvallejo@ugto.mx

* Correspondence: normagut@ugto.mx (N.G.-O.); ramosre@ugto.mx (E.R.-R.); Tel.: +52-473-732-00-06 (ext. 2227) (N.G.-O.); +52-473-732-00-06 (ext. 1457) (E.R.-R.)

Received: 1 February 2019; Accepted: 26 April 2019; Published: 29 April 2019

Abstract: Catalyst-type mixed metal oxides with different compositions and Co/Fe ratios were obtained from layered double hydroxides to be used as heterogeneous catalysts in the production of biodiesel. The effect of the Co/Fe ratio on the precursors of the catalysts was analyzed, considering their thermal, textural and structural properties. The physicochemical properties of the catalysts were determined by thermogravimetric analysis (differential scanning calorimetry and thermogravimetric), X-ray diffraction, Fourier-transform infrared spectroscopy, Scanning Electron Microscopy-Energy Dispersive X-ray spectroscopy and N_2-physisorption. The conversion to biodiesel using the different catalysts obtained was determined by diffuse reflectance infrared Fourier-transform spectroscopy and ^{1}H-Nuclear magnetic resonance spectroscopy, allowing us to correlate the effect of the catalyst composition with the catalytic capacity. The conditions for obtaining biodiesel were optimized by selecting the catalyst and varying the percentage of catalyst, the methanol/oil ratio and the reaction time. The catalysts reached yields of conversion to biodiesel of up to 96% in 20 min of reaction using only 2% catalyst. The catalyst that showed the best catalytic activity contains a mixture of predominant crystalline and amorphous phases of $CoFe_2O_4$ and Na_xCoO_2. The results suggest that cobalt is a determinant in the activity of the catalyst when forming active sites in the crystalline network of mixed oxides for the transesterification of triglycerides, with high conversion capacity and selectivity to biodiesel.

Keywords: Cobalt ferrite; layered double hydroxides; ethylesters; biofuels; hydrotalcite; transesterification

---

1. Introduction

Currently, one of the main challenges facing humanity is to reduce the use of petroleum fuels and increase the production of fuels from low carbon sources [1]. A viable alternative is biofuels, which have the advantages of being easily extractable from biomass, biodegradable, non-toxic and environmentally friendly [2,3]. Biodiesel is a liquid fuel derived from triglycerides of animal, vegetable and even microbial origin [4,5]. Biodiesel can be obtained by a great variety of techniques such as direct mixtures, microemulsions, pyrolysis and transesterification [6]. The transesterification technique is the most used because it is easy to carry out; however, the type of catalyst used is important to ensure that the reaction has direct effects on the efficiency of the process and the quality of the products. The catalysts used can be homogeneous, heterogeneous or enzymatic (Figure 1) [7–9].

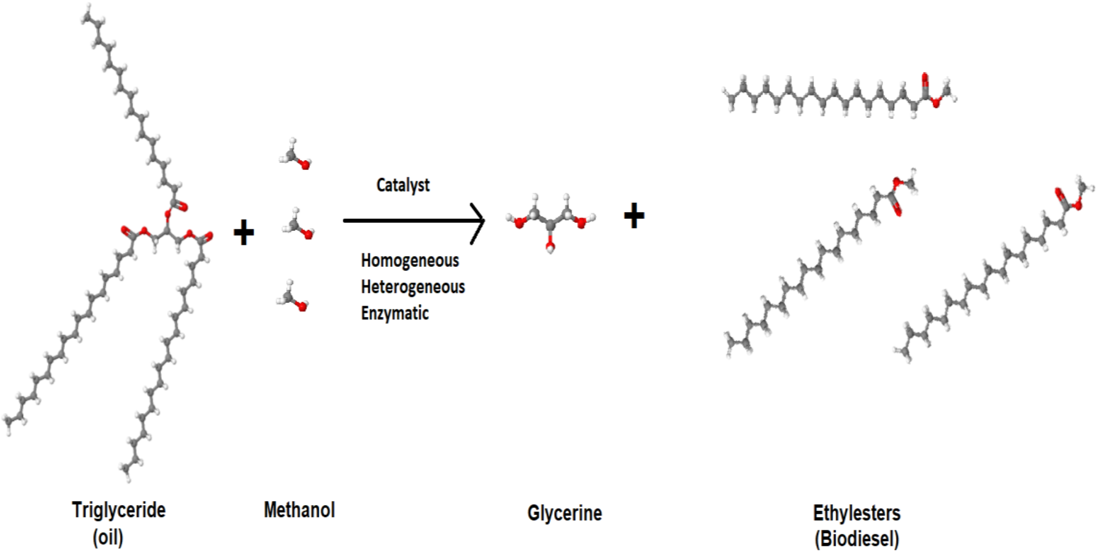

Figure 1. Transesterification reaction for biodiesel production.

Each of the catalytic processes used to obtain biodiesel presents advantages and disadvantages. For example, enzymatic transesterification is considered the most effective and environmentally sustainable method to produce biodiesel; however, its reaction speed is very low, costs are extremely high, and scaling is complicated [10]. Basic homogenous transesterification is easy to operate on an industrial level, has a high catalytic activity and the reaction times are short [11], but has disadvantages, such as that the presence of free fatty acids and water produces soap affecting the entire production process, and that this method generates large volumes of wastewater and therefore has a high environmental impact. On the other hand, heterogeneous catalysts have gained interest in the production of biodiesel, because they are neither consumed nor dissolved in the reaction mixture, which facilitates the separation of the product and the reuse of the catalyst. The main disadvantage of this approach is that it is still in the pilot escape phase and problems of diffusion, immiscibility and mass transfer efficiency are still not resolved at the operational level, which affects the speed of the reaction [12–14].

Recently, the heterogeneous catalysts that have presented greater effectiveness and potential to be used in the production of biodiesel are simple and mixed metal oxides, zeolites, anion exchange resins and carbon-based catalysts, among others [15–20]. Layered double hydroxides (LDH) are a family of natural and synthetic compounds that are characterized by a laminar structure-type hydrotalcite (HT). The sheets are octahedral networks containing metals with divalent and trivalent positive charges that generate a positive residual charge which is neutralized in the presence of anions and water molecules in the interlaminar space. Their molecular formula is $[M^{2+}_{(1-x)}M^{3+}_{x}(OH)_2][A^{n-}]_{x/n}\cdot yH_2O$ [21,22]. Layered double hydroxides can be prepared by different methods such as coprecipitation, hydrolysis with urea, sol–gel, hydrothermal treatment, combustion and mechanical synthesis, among others, with the most common and economic method being coprecipitation [23–25]. Studies have reported that the synthesis method, the conditions of synthesis, the type of cations and structural anions, the metal precursors and the metal ratio M^{2+}/M^{3+} are determining factors on the properties and applications of LDH [26–29]. An important element to improve the catalytic activity of LDH is the thermal treatment to form mixed spinel-type oxides, specifically in the production of biodiesel by heterogeneous catalysis [30,31]. The most relevant studies have shown good results of conversion to biodiesel, but these reactions were found to require a long synthesis time, high temperatures or critical conditions, high percentages of catalyst and large amounts of methanol, among other factors. Table 1 shows examples of investigations in which catalysts of the LDH type have been used, which mainly consist of metals such as Mg, Al, Zn and Fe.

Table 1. Obtaining biodiesel using different layered double hydroxides (LDH)-type catalysts.

Catalyst	Synthesis Conditions	Biodiesel Conversion (%)	References
Mg/Al = 3 HT [1]	Soybean oil:methanol 1:12, 5 wt% of catalyst, at 180 °C, 700 rpm, 180 min, with microwave irradiation	96	Coral, 2019 [30]
Mg/Fe = 5 HT calcined at 500 °C	Rapeseed oil:methanol 1:9, 5% catalyst, 400 rpm at 120 °C for 8 h in Batch autoclave reactor	68	Hajek, 2018 [31]
Comercial Zn/Al = 3.3 HT-KF	Jatropha oil 1:30, 10% catalyst, reflux for 3 h and 30 min in Batch microwave reactor without reporting temperature	50	Fatimah, 2018 [32]
LDH at 300 °C	Oil:alcohol, 50 mg cat:10 mmol oil, 1:30, 65 °C, 3 h	30	Tajuddi, 2018 [33]
Mg/Al = 7 HT at 500 °C	Oil:alcohol 1:48, 6% catalyst, 60 °C, 1 atm, 24 h	92	Navajas, 2018 [34]
Mg/Al = 3 HT at 500 °C	Soybean oil:methanol 1:90, 1000 rpm, 150 °C, 0.4 g cat:0.0045 mol oil, 180 min, autoclave pressure	97	Dhawan, 2018 [35]
Mg/Al = 2 HT nanoparticles at 500 °C	Jatropha oil 1:40, 5%, 3.3–5.5 MPa, 200 °C, 4 h	54	Wang, 2015 [36]
Mg/Al = 3 HT	Soybean oil:methanol 1:14, N_2, 1380 kPa, 115 °C, 4% catalyst, 2 h	95	Prado, 2014 [37]
Mg/Al = 3 HT-10% Fe at 480 °C	Seed oil:methanol 1:6, 1% catalyst, 80 °C, 100 min	96	Macala, 2008 [38]
MgCoAl–LDH at 500 °C	Canola oil: 1:16 methanol, 2% catalyst, 100 °C, 25 atm and 300 min	95	Li, 2009 [39]

[1] HT: hydrotalcite or layered double hydroxide

The above shows a panorama highlighting the need to continue looking for new materials that achieve better efficiencies in the conversion to biodiesel in the shortest possible time and using the smoothest and most controllable reaction conditions.

The modification that has been given to the LDH containing Fe, both in the laminar structure and impregnated, have shown efficient conversion results, but with long reaction times or with systems that require pressure [31,38]. On the other hand, cobalt is a catalytically active element that has been used in many catalytic processes, including transesterification. The use of catalysts with Co content to obtain biodiesel has given interesting results, with the case of the use of materials of type Co(II)-organic compounds in microwave reactors that have reached 80% conversion in 12 h [40]. Other studies have used cobalt supported, for example, in zeolite ZSM5 with in reaction times of 8 h to 95 °C and 80% conversion [41]. Additionally, a study reports the direct esterification of fatty acids to form biodiesel by using a mixture of oxides with Co, Sn and Al with 1:32 oil/methanol ratio, 2% catalyst and 60 °C, reaching 65% conversion in 4 h [42].

The present work focuses on the obtaining of a new catalysts obtained by thermal activation of layered double hydroxides Co/Fe, to be used in the esterification and transesterification reactions to produce biodiesel. The use of Co and Fe as active metals in crystalline networks of the simple and mixed oxides type is proposed, considering mainly that the cobalt is a transition element that can contribute to the formation of active sites for the simultaneous esterification and transesterification of the cooking oil to biodiesel. The effect of the variation of the Co/Fe ratio of the LDH precursor on the physicochemical and catalytic properties of its calcination products at 700 °C for catalytic activation is studied. Complementarily, the best operating conditions for obtaining biodiesel by heterogeneous catalysis were determined, the foregoing to generate a viable alternative for the industrial production of biodiesel under simple operating conditions.

2. Results

2.1. Catalyst Characterization

This section shows the results of the characterization of the catalytic precursors Layered Double Hydroxides (LDH) identified as LDH1, LDH2, LDH3 and LDH4 corresponding to the ratio Co/Fe = 1, 2, 3 and 4 respectively, as well as the products of calcination of LDH identified as MO-LDH1, MO-LDH2, MO-LDH3 and MO-LDH4.

2.1.1. Thermal Evolution of Layered Double Hydroxides (LDH) to Co/Fe-Mixed Oxides (MO-LDH)

Figure 2a shows the thermogravimetric analysis (TGA) of the LDH, corresponding to the different precursors of the mixed Co/Fe oxides. As can be seen, the LDH2 precursor presents a first major weight loss associated with the elimination of water around 200 °C corresponding to 12% of its original weight, while the LDH3 and LDH4 precursors present a weight loss of only 3.5% in that same temperature range. The second weight loss occurs between 600 and 700 °C which for the solid LDH1 amounts to a loss of 22%, LDH2 of 33%, LDH3 of 34.5% and LDH4 of 46.5%, the latter being the highest total loss reached before losing 50% of its mass at 1100 °C. Thermograms by differential scanning calorimetry (DSC) are shown in Figure 2b, where it can be seen that the different Co/Fe precursors synthesized present similar thermal evolutions. The main signals correspond to the dehydration of the molecules housed in the interlaminar at 300 °C and the decarbonation and dehydroxylation at 680 °C associated with the weight loss described in the TGA, which forms the crystalline and amorphous phases of the simple and mixed oxides. In the case of the LDH3 and LDH4 solids, an additional reaction can be seen at 998 °C associated with the sintering of the spinel of the cobalt ferrite ($CoFe_2O_4$).

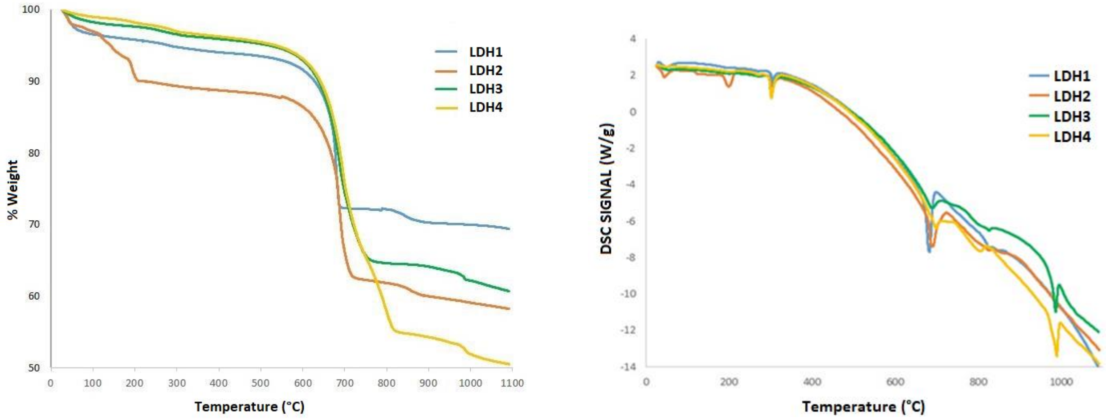

(**a**) (**b**)

Figure 2. Thermal analysis thermograms by differential scanning and thermogravimetric calorimetry of synthesized catalytic precursors: (**a**) thermogravimetric analysis (TGA) and (**b**) differential scanning calorimetry (DSC).

The thermal stability of the LDH synthesized associated with the evolution of the crystalline phases allows us to determine the temperature at which the materials must be activated in order to be used as catalysts in the transesterification of triglycerides to biodiesel. This temperature was found to be 700 °C for the transition of the phases.

2.1.2. Modification of Functional Groups by Thermal Activation of the Catalyst

Figure 3 shows the FTIR spectra of the LDHs prior to activation (Figure 3a) compared to the spectra of the catalysts obtained by calcination at 700 °C (Figure 3b). As can be seen, the thermal decomposition profiles are correlated to the activation temperature of the catalysts. A broad band of low intensity close to 3300 cm^{-1} can be observed in all spectra of Figure 3b, which is associated with hydroxyl groups, where in the case of the catalysts MO-LDH1 and MO-LDH2 it is a double band associated with the interaction of hydroxyl and carbonates that could be reabsorbed on the surface given the precursor reconstruction effect. This signal attributed to the hydroxyl groups is of low intensity for the catalysts MO-LDH3 and MO-LDH4. With respect to the presence of carbonate groups, these signals are observed between 1200 and 1600 cm^{-1}. In the case of MO-LDH1 the band belonging to carbonates is not observed, for MO-LDH2 most of the carbonates are interlaminar, in the MO-LDH3 the carbonates are free, that is, they are adsorbed on the surface and the MO-LDH4 carbonates are not observed. For the case of the modifications in the interlaminar bonds of the metals when evolving from hydroxides to oxides, these signals can be identified in the region between 400 and 1000 cm^{-1}. For the catalyst MO-LDH3 and MO-LDH4, more intense bands can be observed that belong to the Fe–O, Co–O and Fe–O–Co bonds, these signals are characteristic of an infrared spectrum of the cobalt ferrite. which are less intense for the catalysts MO-LDH1 and MO-LDH2 given the over positioning some signals of simple and mixed oxides.

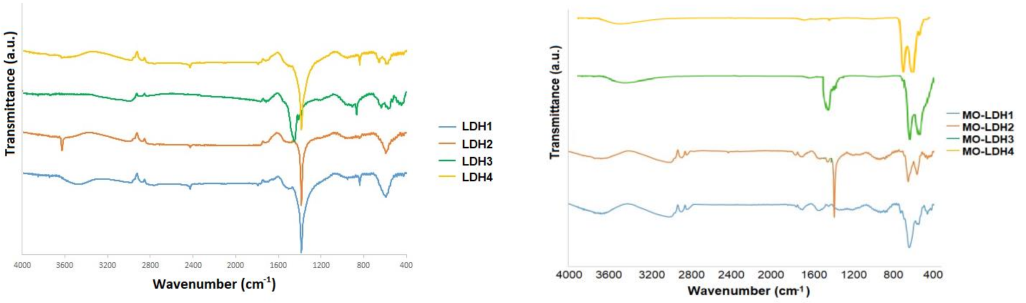

(**a**) (**b**)

Figure 3. Spectra of infrared spectroscopy of the catalysts: (**a**) LDH synthesized and (**b**) LDH calcined at 700 °C.

2.1.3. Identification of Crystalline Phases Present in the Catalysts

Figure 4 shows the X-ray diffraction patterns of the catalysts obtained by calcination at 700 °C. The solid MO-LDH1 does not present the crystalline phase of $CoFe_2O_4$ (cobalt ferrite) but many noise signals associated with amorphous phases. This confirms our observations of the infrared spectra, showing that when cobalt ferrite is present it is still amorphous, in addition to the presence of small crystalline phases secreted by Fe_3O_4, CoO and CoO_2. The solid MO-LDH2 can be observed in the presence of the crystalline phase of $CoFe_2O_4$ accompanied by segregated phases of Fe_3O_4, CoO_2 and CoO. In the case of solid MO-LDH3, a better crystallinity of $CoFe_2O_4$ is observed, as evidenced in the FTIR spectra, in addition to the presence of a segregated phase of CoO_2 and $CoNa_xO_2$. In the case of MO-LDH4, the $CoFe_2O_4$ phase is observed, combined with CoNaxO$_2$, CoO_2 and CoO [43,44].

For the solids MO-LDH3 and MO-LDH4, the presence of sodium in the crystalline networks is due to the fact that the amount of iron is less than cobalt, which allows cobalt to interact with sodium at the moment of synthesis in basic medium, favoring the integration of sodium in the crystalline network and modifying the properties of the catalysts.

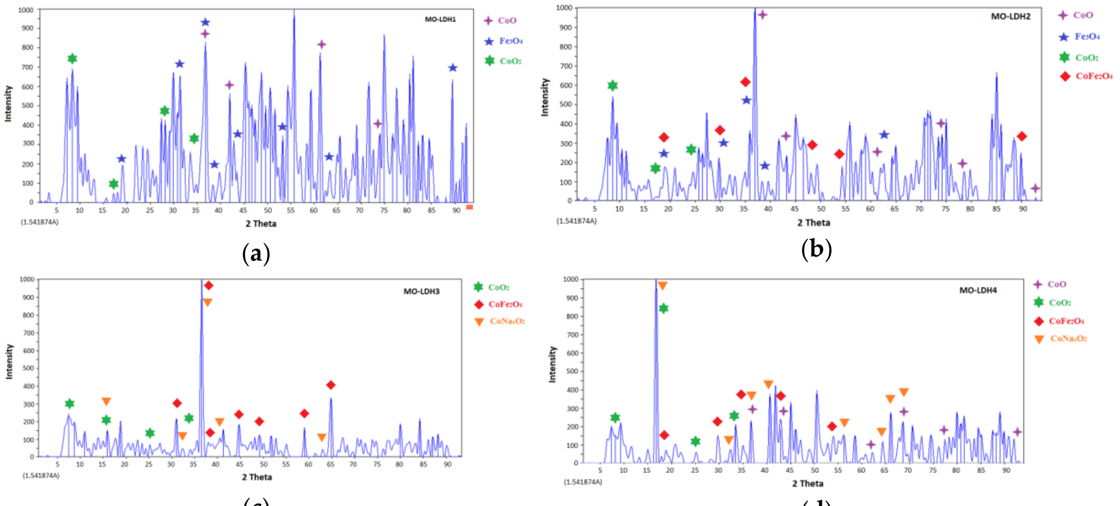

(**a**) (**b**)

(**c**) (**d**)

Figure 4. X-ray diffraction patterns of the catalysts obtained at 700 ° C: (**a**) MO-LDH1, (**b**) MO-LDH2, (**c**) MO-LDH3 and (**d**) MO-LDH4.

Given the variation in the composition and segregation of the crystalline phases in the different catalysts obtained from the calcination products at 700 °C of the layered double hydroxides with different Co/Fe molar ratio, the effect of the presence may be analyzed of the different simple and mixed oxides of Co and Fe with respect to the catalytic activity.

2.1.4. Determination of Textural Properties of the Catalysts

Figure 5 shows the physisorption isotherms of N_2 for the catalysts obtained by calcination at 700 °C. The adsorption isotherms for all solids belong to type III, corresponding to physical adsorption in multilayers by a free surface, which is characteristic of macroporous solids (pore size greater than 50 nm). However, a variation in the curl of hysteresis was observed, especially for the solid MO-LDH1. The reason why the solid MO-LDH1 presents a broad curl is associated with an incomplete thermal evolution so that it does not yet collapse the structure of the oxides. The rest of the catalysts show narrow curls, which reflect a collapse of the interlaminar spaces associated with a decrease in the specific area.

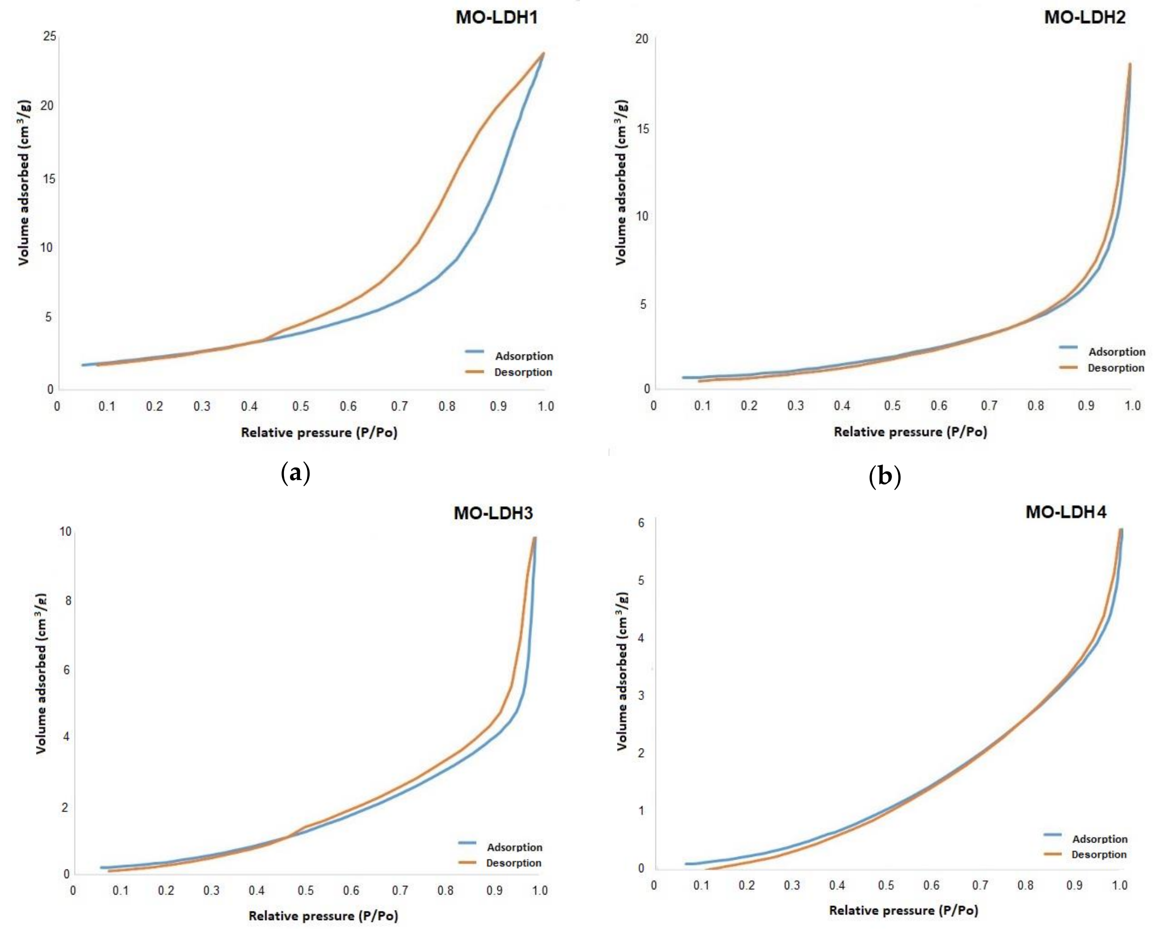

(**a**) (**b**)

(**c**) (**d**)

Figure 5. Isotherms of the physisorption of N_2 of the catalysts obtained at 700 °C: (**a**) MO-LDH1, (**b**) MO-LDH2, (**c**) MO-LDH3 and (**d**) MO-LDH4.

Table 2 shows the results of the textural characterization of mixed oxides of different molar ratios: Brunauer, Emmett and Teller (BET)-area, diameter and pore volume.

Table 2. Textural properties of the catalysts obtained at 700 °C.

Catalyst	BET-Area (m^2/g)	Pore Diameter (nm)	Pore Volume (cm^3/g)
MO-LDH1	8.37	83	0.031
MO-LDH2	3.18	38	0.009
MO-LDH3	2.92	54	0.007
MO-LDH4	1.48	61	0.006

As can be seen, the catalysts show a trend of the value of the specific area in correlation with the metal molar ratio Co/Fe and with the thermal decomposition profile of the catalysts. For all cases the areas are less than 10 m^2/g, which suggests the degree of collapse of the laminar structure associated with thermal evolution to simple and mixed metal oxides. In relation to the pore diameter, only the MO-LDH2 catalyst has mesoporous size, and the rest exhibit a larger size corresponding to macropores.

2.1.5. Surface Analysis of the Particles of the Catalysts

Figure 6 shows the photographs obtained by scanning electron microscopy of the catalysts. As can be observed, the solid MO-LDH1 and MO-LDH2 show an amorphous texture with the presence of few hexagonal crystalline structures, which is because the crystallization by thermal evolution has not concluded for all the crystalline phases of the mixed and simple oxides. For the solids MO-LDH3 and MO-LDH4, the presence of hexagonal particles in cumulus and in the form of thin, defined sheets increases markedly. The hexagonal sheets form due to the large amount of mixed oxide Co/Fe present in the different catalysts, mainly in the MO-LDH3 catalyst. In the case of the MO-LDH4 catalyst, very large hexagonal prisms resulting from the ordering of the catalyst sheets can be clearly observed.

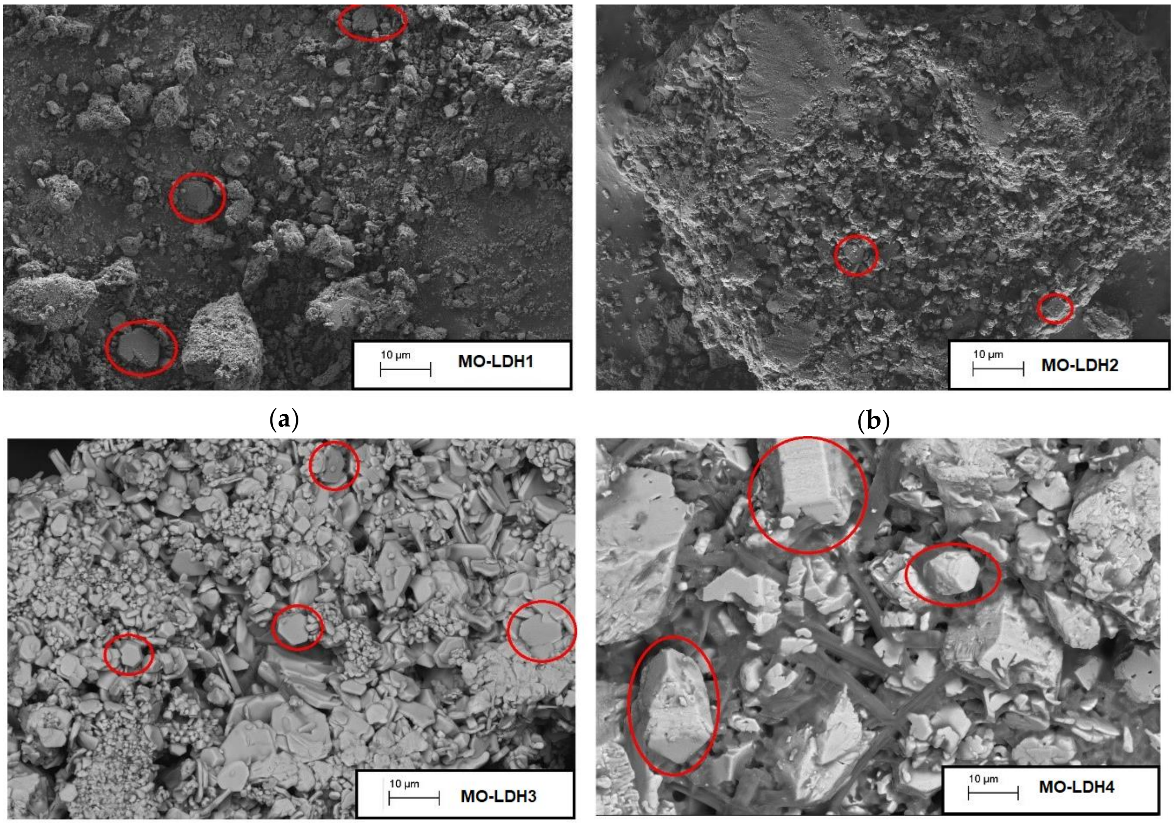

(**a**) (**b**)

(**c**) (**d**)

Figure 6. Scanning microscopy images of the catalysts obtained at 700 °C: (**a**) MO-LDH1, (**b**) MO-LDH2, (**c**) MO-LDH3 and (**d**) MO-LDH4.

2.1.6. Elemental Composition on the Surface of the Particles

Finally, in Figure 7 is shown an elemental analysis performed on the catalysts obtained by calcination at 700 °C. As can be seen, the general composition of the mixed oxides is similar for all the catalysts, which was to be expected because they were synthesized with the same methodology. The variation between the catalysts lies in the variation in the metallic Co/Fe ratio in the synthesis of the catalytic precursors, as well as in the proportion of the simple and mixed metal oxides present in the catalyst. The elements present in the catalysts are: cobalt, iron, sodium, oxygen and carbon, where by correlation with the diffractograms are in the form of metal oxides for the case of cobalt, iron and sodium; whereas the carbon by confirmation of the FTIR spectra corresponds to the CO_2 physisorbed on the surface of the catalysts.

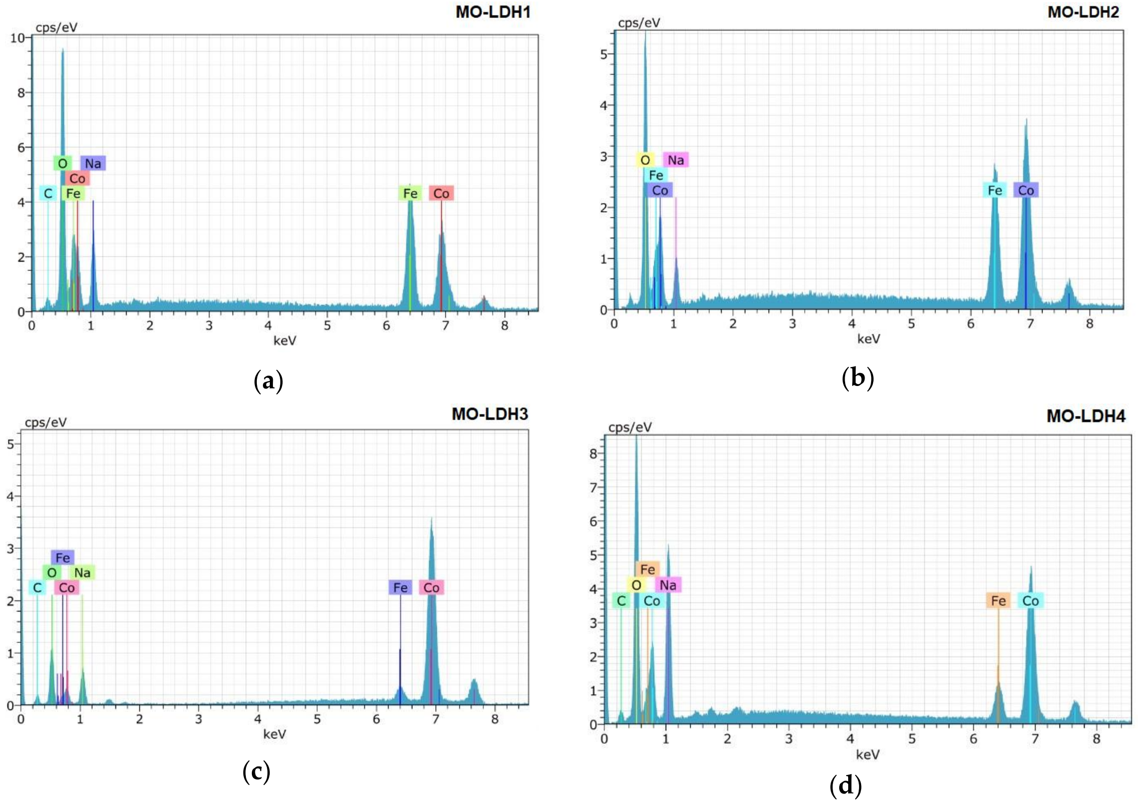

(**a**) (**b**) (**c**) (**d**)

Figure 7. Elemental analysis of the catalysts obtained at 700 °C: (**a**) MO-LDH1, (**b**) MO-LDH2, (**c**) MO-LDH3 and (**d**) MO-LDH4.

Table 3 shows the results of the determination of the Co/Fe molar ratio in the catalytic precursors compared with that of the catalysts.

Table 3. Comparison of the variation of the Co/Fe molar ratio on the surface of the precursor particles and their corresponding mixed oxides.

Sample	Molar Ratio	Sample	Molar Ratio
LDH1	1.04	MO-LDH1	0.85
LDH2	1.85	MO-LDH2	1.94
LDH3	2.45	MO-LDH3	3.93
LDH4	4.10	MO-LDH4	5.63

As can be seen, for the case of catalytic precursors, the theoretical molar ratio of Co/Fe is very close to the values of the molar ratio calculated from the average quantification on the surface of the particles. After the heat treatment, it can be seen that for the case of the MO-LDH1 and MO-LDH2 solids the Co/Fe ratio varies very little, which can be attributed to the homogeneity of the dispersion of metals in the particles. These solids were also homogeneous after thermal evolution. In the case of the MO-LDH3 and MO-LDH4 catalysts, a decrease in the Co/Fe molar ratio is observed, which can be attributed to the fact that the particles are more crystalline with defined edges, which concentrate the iron in the crystalline network, thus decreasing the amount of iron on the surface.

2.2. Evaluation of Biodiesel Quality

The physical and rapid qualitative parameter that was used to determine whether transesterification was performed for the conversion of triglycerides to biodiesel was the kinematic viscosity, starting from the fact that the oil prior to transesterification had a viscosity of 32 cp, while biodiesel with a high percentage of conversion presents values below 6 cp according to ASTMD6751, implying that a decrease in viscosity is associated with the transesterification of the fatty acids present in the oil [45].

Once it was confirmed that the viscosity had been reduced to values close to the norm, we proceeded to the quantification and confirmation of the conversion by diffuse reflectance infrared Fourier-transform spectroscopy (DRIFTS) and ^{1}H-Nuclear magnetic resonance (NMR) spectroscopy [46], as well as the verification of the international parameters of density, corrosion of the copper foil and turbidity. These parameters can be used to verify the feasibility of the products' application as biofuels in internal combustion engines.

Table 4 shows the best conversion percentages obtained in the shortest reaction times tested for obtaining biodiesel using a 3% catalyst, a molar oil/methanol ratio of 1:12, a reaction temperature of 65 °C and constant agitation at 1400 rpm.

Table 4. Quality parameters of biodiesel obtained using the different catalysts.

Catalyst	**Time (min)**	**Viscosity (cp)**	**Density (kg/m^3)**	**Acidity Index (mg$_{KOH}$/g)**	**Corrosion of Copper Foil**	**Turbidity (°C)**	**DRIFTS Conversion (%)**	**^{1}H-NMR Conversion (%)**
MO-LDH1	60	6.92 ± 0.3	885 ± 6	0.18	1a	<1	70.4 ± 3.4	63.3
MO-LDH2	60	6.55 ± 0.1	883 ± 5	0.20	1a	<1	80.1 ± 3.4	82.0
MO-LDH3	30	3.71 ± 0.2	881 ± 2	0.19	1b	<1	93.2 ± 3.3	92.7
MO-LDH4	30	3.66 ± 0.1	875 ± 5	0.20	1a	<1	96.2 ± 3.4	96.0

It can be seen that the four catalysts achieved a conversion of triglycerides to biodiesel by lowering the viscosity of the 32 cp oil to values lower than 7 cp. In the case of the MO-LDH1 and MO-LDH2 catalysts, at a reaction time of 30 min, the viscosities were 14.24 and 15.27 cp, respectively, which indicated that the conversion had not yet finished. When the reaction time was extended to 60 min, a decrease in viscosity values close to 7 cp was observed, associated with conversion values greater than 70%. On the other hand, for the case of the MO-LDH3 and MO-LDH4 catalysts, at 30 min they had already reached viscosities below 4 cp and achieved conversions greater than 90%.

Figure 8 shows the ^{1}H-NMR spectra which were used to calculate the % conversion to biodiesel from the M signal corresponding to the methyl group of the biodiesel methylesters that is formed as the reaction is carried out. Associated with the M signal is the G zone corresponding to the monoglycerides, diglycerides and triglycerides of the oil, which disappear in the conversion to methylesters.

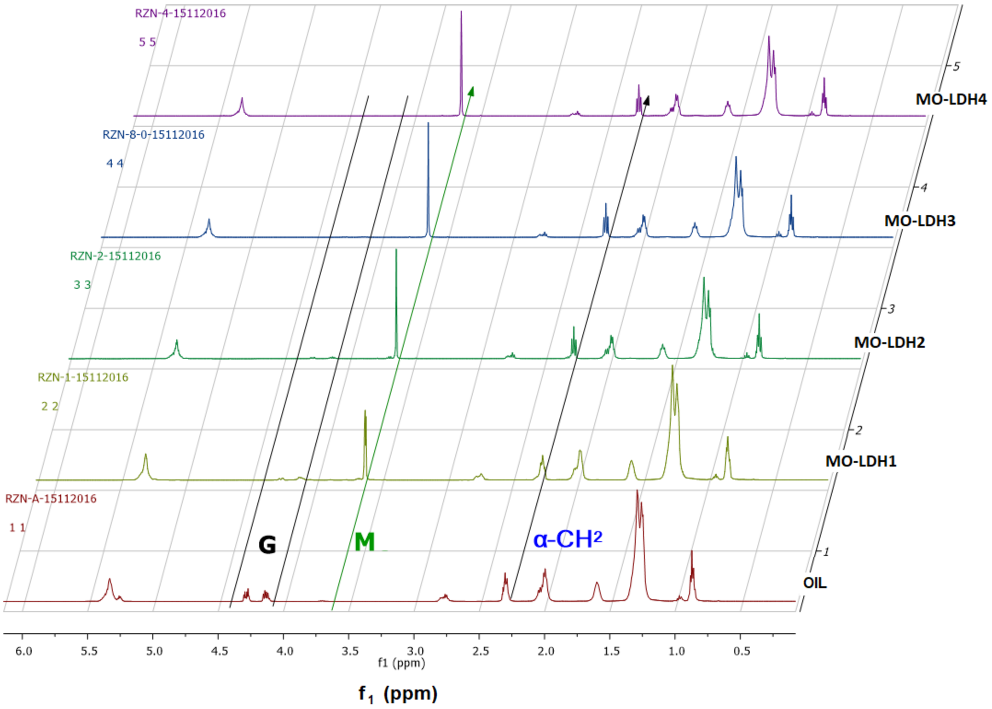

Figure 8. Nuclear magnetic resonance spectra of ^{1}H in the transesterification reaction for biodiesel production as a function of reaction time.

With this analysis it can be verified that at 60 min the MO-LDH1 and MO-LDH2 catalysts have not yet been able to complete the transesterification reaction of all triglycerides in the oil, but there is a high percentage of conversion greater than 60%. It can be observed that in the case of the MO-LDH1 catalyst, the activity reached at 60 min was 63.3%, which can be attributed to the fact that it consists of particles of amorphous material with a small amount of simple CoO, CoO_2 and Fe_3O_4, which provide a greater specific area than the rest of the catalysts, but with fewer active sites for catalytic conversion. The MO-LDH2 catalyst has a better conversion capacity, reaching 82% in 60 min, because the catalyst contains the mixed oxide $CoFe_2O_4$ in addition to the segregated phases of Fe_3O_4, CoO_2 and CoO. For the case of the MO-LDH3 and MO-LDH4 catalysts, a high conversion to biodiesel with values of 92.7% and 96%, respectively, can be observed. In the NMR spectra it can be observed that there are no signals in the G zone, which implies that they have already completed the transesterification reaction for the formation of the methyl esters when a high intensity of the corresponding M signal is observed. This is associated with better conversion capacity of the MO-LDH3 and MO-LDH4 catalysts, attributed to the presence of crystalline particles of the mixed oxides $CoFe_2O_4$ and $CoNa_xO_2$.

With respect to the complementary quality parameters shown in Table 4, related to the acidity index, corrosion of the sheet and turbidity of the biodiesels obtained with the MO-LDH3 and MO-LDH4 catalysts, it can be seen that these parameters are within the standard ranges. Thus, it is confirmed that the biodiesel obtained with these catalysts can be used in an internal combustion engine.

As the MO-LDH4 catalyst exhibits a better conversion capacity, reaching 96% and presenting a viscosity decrease to 3.66 cp, this catalyst was used to correlate and improve the reaction conditions for obtaining biodiesel with respect to the decrease of the reaction time, the amount of catalyst and the aomount of methanol used in the synthesis.

In relation to the reaction time, a study of the conversion capacity of the catalyst as a function of time was carried out, from 5 to 30 min, while maintaining the reaction conditions of 3% catalyst, a molar ratio of oil/methanol of 1:12, a reaction temperature of 65 °C and constant stirring at 1400 rpm. Table 5 shows the results of the biodiesel conversion values quantified by ^{1}H-NMR obtained with the catalyst MO-LDH4 at times below 30 min, also indicating the viscosity values as a quality parameter of the biodiesel.

Table 5. Percentage of conversion of the biodiesel obtained with the MO-LDH4 catalyst at different reaction times.

Time (min)	Viscosity (cp)	^{1}H-NMR Conversion (%)
5	4.14	81.33
10	3.67	89.33
15	3.26	90.00
20	3.43	94.00
25	2.88	91.33
30	3.22	96.00

It can be seen that the MO-LDH4 catalyst has the capacity to convert the oil to biodiesel in only 5 min with viscosity values that comply with the norm, reaching a conversion of 81%. These results exceed the capacity found for the MO-LDH2 catalyst, which required 60 min to reach the same conversion capacity, thus confirming the fast selectivity and conversion capacity of the catalyst as well as the important role of mixed oxides in the process. After 5 min, the biodiesel complies with the viscosity quality parameter. With respect to the variation of the conversion% as a function of time, it can be seen that from 5 to 30 min the values of the conversion increase gradually from 81.3% to 96%. The activity of the MO-LDH4 catalyst, attributed to the presence of particles of the mixed oxides $CoFe_2O_4$ and $CoNa_xO_2$ and of the simple oxides CoO_2 and CoO, is favored by the crystalline structure of the catalyst particles, as well as by the macroporosity that allows access to active sites. An advantage of the catalyst is that the formation of catalytically active sites is favored by the formation of mixed crystalline structures.

The combination of the different particles containing Co species with different oxidation states in both the simple oxides and in the mixed with Fe and Na, as a catalytic composition, allows the formation of different acidic and basic sites for the esterification of the free fatty acids present in the oil, as well as for the transesterification of the fatty acids from triglycerides to biodiesel. The process that could be developing in the catalyst is proposed based on the recent kinetic model of transesterification in two sites of the Eley–Rideal type, where the mechanism has three important steps, the first step is the adsorption of both methanol and oil on the surface of the catalyst, in the second step a tetrahedral intermediate is produced from the alkoxide group which attacks the positively polarized carbon of the triacylglyceride in both the liquid phase and the catalyst surface, and the third step involves the production of a fatty acid ester and the release of a diacylglycerides. this procedure is repeated with the following two fatty acids bound to the glycerol [47].

Table 6 shows the viscosity values obtained by decreasing the amount of methanol used in the synthesis while preserving the synthesis conditions of 3% catalyst, a reaction temperature of 65 °C, constant agitation at 1400 rpm and a reaction time of 30 min. It can be seen that the efficiency of the catalyst is not significantly affected by decreasing the oil/methanol ratio from 1:12 to 1:9 and to 1:6. This represents an operational advantage since an excess of methanol as a reagent is not required to displace the reaction to products, as in most procedures reported by heterogeneous catalysis [8,22]. In this case, the conversion capacity is even slightly improved by decreasing the volume of methanol in the reaction.

Table 6. Percentage of conversion of the biodiesel obtained with the MO-LDH4 catalyst at different oil/methanol ratios.

Molar ratio	**Viscosity (cp)**	**^{1}H-NMR Conversion (%)**
6	3.43	96
9	3.51	96
12	3.57	95

The effect of the decrease of the amount of the catalyst used in the transesterification reaction was tested, while maintaining the conditions of a reaction temperature of 65 °C, an oil/ethanol molar ratio of 1:12, constant agitation at 1400 rpm and a reaction time of 30 min. Table 7 shows that the efficiency of the process is not significantly affected by decreasing the amount of the catalyst from 3 to 2%, allowing a reduction of up to one third of the catalyst.

Table 7. Percentage of conversion of the biodiesel obtained with the MO-LDH4 catalyst at different oil/methanol ratios.

% Catalyst	**Viscosity (cp)**	**^{1}H-NMR Conversion (%)**
1	5.27	90
2	3.52	95
3	3.57	96

Finally, to verify the best synthesis conditions considering the simultaneous decrease of the catalyst, methanol and reaction time, biodiesel was obtained with 2% catalyst, a oil/methanol molar ratio of 1:6 and a reaction time of 20 min. Thus, we achieved a biodiesel with quality parameters that comply with the ASTM standards, as reported in Table 8.

Table 8. Quality parameters of the biodiesel obtained using the MO-LDH4 catalyst under optimal synthesis conditions.

Parameters	**Limits ASTM**	**Biodiesel Obtained**
Density (kg/m^{3})	860–900	884
Viscosity (cp)	1.9–6.0	3.89
Corrosion of copper foil	1 class	1 class
Acidity index (mg$_{KOH}$/g)	0.5	0.2
Turbity	not established	<1
% of biodiesel conversion	not established	90.24%
Methylester composition by Gas Chromatography-Flame Ionization Detector (GC-FID)	not established	C18:1 ^{9C}, C18:2 ^{9C,12C}, C18:3 ^{9C,12C,15C}

It can be seen that the biodiesel obtained by Gas Chromatography-Flame Ionization Detector (CG-FID) is mainly composed of the methyl esters of oleic acid (C18: 1 cis-9), linoleic acid (C18: 2 cis-9,12) and linolenic acid (C18: 3 cis-9,12,15), and in a lower proportion of palmitic acid (C16: 0) and stearic acid (C18: 0), which were identified according to the chromatograms shown in Figure 9. These results confirm the high selectivity of MO-LDH4 towards unsaturated fatty acids.

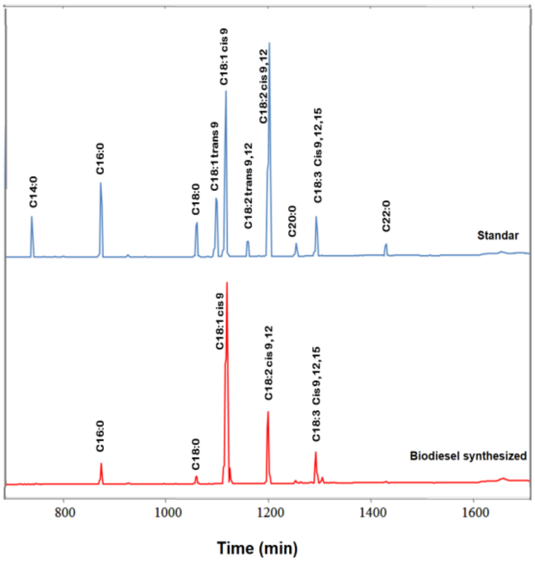

Figure 9. Chromatograms of biodiesel obtained with 2% MO-LDH4 catalyst compared to the Supelco standard for Fatty Acid Methyl Esters (FAME).

The results of the analysis of the biodiesel composition obtained confirm the formation of the methyl esters of the respective fatty acids that formed the oil used as raw material in the transesterification reaction. The biodiesel obtained complies with the quality standards set by the ASTM international standards. The quality of the biodiesel was improved by the selectivity and high conversion capacity of the catalyst.

3. Materials and Methods

3.1. Synthesis of the Catalyst

The catalysts were synthesized by the procedure registered in the patent process MX2015009362 of the Mexican Institute of Industrial Property [48], as described below. A series of Co/Fe layered double hydroxides samples was prepared by the coprecipitation method with a molar ratio $Co^{2+}/Fe^{3+} = 1$, 2, 3 and 4 using a stoichiometric amount of cobalt nitrate hexahydrate and iron nitrate nonahydrate. The aqueous solutions containing the metal salts were coprecipitated in a basic medium with an alkaline solution of sodium hydroxide (2M) and sodium bicarbonate (1M) at a constant pH of 11.5. After complete precipitation of the mixture, the precipitates were washed with water at room temperature until obtaining a pH of 9. Subsequently the precipitates were dried in an oven at 70 °C for 24 h to obtain the LDH as catalytic precursors. The materials were identified as LDH1, LDH2, LDH3 and LDH4 corresponding to the Co/Fe ratio = 1, 2, 3 and 4 respectively. The catalytically active phases were obtained by calcination of the precursors at 700 °C for 4 h. The calcination products of the layered doble hydroxides were identified as corresponding MO-LDH1, MO-LDH2, MO-LDH3 and MO-LDH4.

3.2. Physicochemical Characterization of the Catalyst

The catalysts were characterized by (a) differential scanning calorimetry (DSC) and thermogravimetric analysis (TGA) with a Universal (Irapuato, Mexico) V4.5A TA Instruments: SDT Q600 V20.5 Build 15; (b) X-ray powder diffraction (XRD) in Inel Equinox (Guanajuato, Mexico) with an X-ray tube coupled with a copper anode using monochromatic CuKα radiation; (c) Fourier transform infrared spectroscopy (FTIR) in a Bruker Tensor (Guanajuato, Mexico) 27 with OPUS software version 6.5; (d) textural properties in an ASAP (Guanajuato, Mexico) 2010 and (e) scanning electron microscopy (SEM) using an X Carl Zeiss Evo (Guanajuato, Mexico) HD-15 microscope with an integrated X-ray dispersive energy microanalysis system.

3.3. Production of Biodiesel

The production of biodiesel was developed by the procedure registered in the patent process MX2015009362 of the Mexican Institute of Industrial Property [48], as described below. To obtain biodiesel, a batch reactor was used with the operating conditions in a reflux system at 65 °C, constant agitation at 1400 rpm and a pressure atmosphere. The alcohol used in the synthesis was anhydrous methanol (Golden Bell, Guadalajara, Mexico) and the source of triglycerides was commercial cooking oil. The variables used in the synthesis of biodiesel were the oil/methanol molar ratio (1:6, 1:9 and 1:12), the percentage of oil/catalyst (1, 2 and 3% w/w) and the reaction time (30 and 60 min). Initially, 3 g of calcined LDH was added to 50 mL methanol in a 500 mL three-necked glass flask equipped with a reflux condenser. The mixture was vigorously mixed under atmospheric and heated until the temperature reached 50 °C. Then, 100 mL of cooking oil, was added to the reactor and the temperature was increased to 65 °C. The mixture was stirred at 1400 rpm during the reaction time (30 min). At the end of the reaction, methanol was recovered by evaporation, catalyst was recovered by vacuum filtration, and subsequently, glycerol, and biodiesel were separated by decantation.

3.4. Evaluation of the Quality of Biodiesel

The quality parameters of the biodiesel were evaluated in accordance with the ASTM international standards to verify that the quality indicated in the ASTM D6751 standard was met. The viscosity was determined in accordance with ASTM D445. The density was determined according to ASTM D121718. The ASTM D66419 standard was used for the acidity index. The corrosion of copper foil was evaluated according to ASTM D13020. Turbidity was measured according to ASTM 250021. The quantification of the conversion of biodiesel by FTIR with diffuse reflectivity (DRIFTS) was conducted as established in ASTM D7371, as well as by proton nuclear magnetic resonance (^{1}H-MNR). The determination of the methyl esters contained in the biodiesel was carried out in accordance with the ASTM D6584 standard.

4. Conclusions

Catalytic precursors of the layered double hydroxides type with different Co/Fe ratios were synthesized in a basic medium, which allowed us to obtain catalysts that showed a correlation between their physicochemical properties and their catalytic capacity in the conversion of triglycerides to biodiesel. The best conversion capacity was presented by the MO-LDH4 catalyst with a 96% conversion to biodiesel by transesterification using a molar alcohol/oil ratio of 6:1, with a reaction time of 20 min and the catalyst percentage of 2%, mainly formed by a mixture of crystalline particles in the form of stacked sheets. The high capacity and selectivity for the conversion of triglycerides to biodiesel shown by the MO-LDH4 catalyst is attributed to the fact that it is a composite catalyst that contains a combination of the simple oxides CoO_2 and CoO and the mixed oxides $CoFe_2O_4$ and $CoNa_xO_2$ where the Co with different oxidation states in combination with O, Fe and Na, favors the presence of acidic and basic sites for the transesterification esterification of the oil to biodiesel.

5. Patents

MX2015009362 Esthela Ramos Ramírez, Norma Leticia Gutiérrez-Ortega, José de Jesús Monjaraz Vallejo, "Obtaining Cobalt Ferrite for its application as a catalyst in the optimization of esterification and transesterification reactions of fatty acids for the biodiesel production process" ("Obtención de Ferrita de Cobalto para su aplicación como catalizador en la optimización de las reacciones de esterificación y transesterificación de ácidos grasos para el proceso de producción de biodiesel" titule in spanish), request patent filed with the Mexican Institute of Industrial Property (IMPI Spanish acronym) Publication date: January 20, 2017.

Author Contributions: Conceptualization, G.-O.N. and R.-R.E.; methodology, G.-O.N. and M.-V.J.; validation, G.-O.N. and R.-R.E.; formal analysis, S.-M.A.; investigation, Z.-M.A.; resources, S.-M.A.; data curation, Z.-M.A.;

writing—original draft preparation, G.-O.N.; writing—review and editing, R.-R.E.; project administration, R.-R.E.; funding acquisition, G.-O.N.

Funding: This research received no external funding. Funding was received from the resources of the university of Guanajuato.

Acknowledgments: This work was supported by the Professors Improvement Program (PROMEP Spanish acronym) of the Public Education Secretary (SEP Spanish acronym), and the Direction of Research and Postgraduate Course Support (DAIP Spanish acronym) from the University of Guanajuato. The authors thank the Directorate of Research Support and the Postgraduate Program of the University of Guanajuato for funding and CONACYT for the scholarship received for the completion of postgraduate studies. In addition, Dr. Ramón Zarraga and Dr. Ricardo Navarro from the University of Guanajuato are thanked for the support with the NMR and SEM-EDX techniques, respectively.

Conflicts of Interest: The authors declare no conflict of interest.

References

1. Oliveira, F.C.; Coelho, S.T. History, evolution, and environmental impact of biodiesel in Brazil: A review. *Renew. Sust. Energ. Rev.* **2017**, *75*, 168–179. [CrossRef]
2. García-Olivares, A.; Ballabrera-Poy, J. Energy and mineral peaks, and a future steady state economy. *Technol. Forecast. Soc. Change* **2015**, *95*, 587–598. [CrossRef]
3. Oh, Y.K. Recent developments and key barriers to advanced biofuels: A short review. *Bioresour. Technol.* **2018**. [CrossRef]
4. Semwal, S.; Arora, A.K.; Badoni, R.P.; Tuli, D.K. Biodiesel production using heterogeneous catalysts. *Bioresour. Technol.* **2011**, *102*, 2151–2161. [CrossRef] [PubMed]
5. Natarajan, Y.; Nabera, A.; Salike, S.; Tamilkkuricil, V.D.; Pandian, S.; Karuppan, M.; Appusamy, A. An overview on the process intensification of microchannel reactors for biodiesel production. *Chem. Eng. Process.* **2019**, *136*, 163–176. [CrossRef]
6. Ge, J.C.; Yoon, S.K.; Choi, N.J. Using Canola Oil Biodiesel as an Alternative Fuel in Diesel Engines: A Review. *Appl. Sci.* **2017**, *7*, 881. [CrossRef]
7. Tariq, M.; Al, S.; Khalid, N. Activity of homogeneous and heterogeneous catalysts, spectroscopic and chromatographic characterization of biodiesel: A review. *Renew. Sust. Energ. Rev.* **2012**, *16*, 6303–6316. [CrossRef]
8. Shan, R.; Lu, L.; Shi, Y.; Yuan, H.; Shi, J. Catalysts from renewable resources for biodiesel production. *J. Energ. Conver. Manage.* **2018**, *178*, 277–289. [CrossRef]
9. Chang, C.C.; Teng, S.; Yuan, M.H.; Ji, D.R.; Chang, C.Y.; Chen, Y.H.; Shie, J.L.; Ho, C.; Tian, S.Y.; Andrade-Tacca, C.A.; et al. Esterification of Jatropha Oil with Isopropanol via Ultrasonic Irradiation. *Energies* **2018**, *11*, 1456. [CrossRef]
10. Christopher, L.P.; Kumar, H.; Zambare, V.P. Enzymatic biodiesel: Challenges and opportunities. *Appl. Energ.* **2014**, *119*, 497–520. [CrossRef]
11. Reyero, I.; Arzamendi, G.; Zabala, S.; Gandía, L.M. Fuel Kinetics of the NaOH-catalyzed transesterification of sunflower oil with ethanol to produce biodiesel. *Process. Technol.* **2015**, *129*, 147–155. [CrossRef]
12. Abdullah, S.H.Y.S.; Hanapi, N.H.M.; Azid, A.; Umar, R.; Juahir, H.; Khatoon, H.; Endut, A. A review of biomass-derived heterogeneous catalyst for a sustainable biodiesel production. *Renew. Sust. Energ. Rev.* **2017**, *70*, 1040–1051. [CrossRef]
13. Yan, S.; Maggio, C.D.; Mohan, S.; Kim, M.; Salley, S.O.; Simon, K.Y. Advancements in Heterogeneous Catalysis for Biodiesel Synthesis. *Top. Catal.* **2010**, *53*, 721–736. [CrossRef]
14. Dimian, A.C.; Srokol, Z.W.; Mittelmeijer-Hazeleger, M.C.; Rothenberg, G. Interrelation of Chemistry and Process Design in Biodiesel Manufacturing by Heterogeneous Catalysis. *Top. Catal.* **2010**, *53*, 1197–1201. [CrossRef]
15. Chouhan, A.P.S.; Sarma, A.K. Modern heterogeneous catalysts for biodiesel production: A comprehensive review. *Renew. Sust. Energ. Rev.* **2011**, *15*, 4378–4399. [CrossRef]
16. Lee, H.V.; Juan, J.C.; Hin, T.Y.Y.; Ong, H.C. Environment-Friendly Heterogeneous Alkaline-Based Mixed Metal Oxide Catalysts for Biodiesel Production. *Energies* **2016**, *9*, 611. [CrossRef]

17. Chang, K.L.; Lin, Y.C.; Jhang, S.R.; Cheng, W.L.; Chen, S.C.; Mao, S.Y. Rapid Jatropha-Castor Biodiesel Production with Microwave Heating and a Heterogeneous Base Catalyst Nano-Ca(OH)$_2$/Fe$_3$O$_4$. *Catalysts* **2017**, *7*, 203. [CrossRef]
18. Du, L.; Ding, S.; Li, Z.; Lv, E.; Lu, J.; Ding, J. Transesterification of castor oil to biodiesel using NaY zeolite-supported La$_2$O$_3$ catalysts. *Energ. Convers. Manage.* **2018**, *173*, 728–734. [CrossRef]
19. Jaya, N.; Selvan, B.K.; Vennison, S.J. Synthesis of biodiesel from pongamia oil using heterogeneous ion-exchange resin catalyst. *Ecotox. Environ. Safe.* **2015**, *121*, 3–9. [CrossRef]
20. Tanga, Z.E.; Lima, S.; Panga, Y.L.; Ongb, H.C.; Lee, K.T. Synthesis of biomass as heterogeneous catalyst for application in biodiesel production: State of the art and fundamental review. *Renew. Sust. Energ. Rev.* **2018**, *92*, 235–253. [CrossRef]
21. Cavani, F.; Trifiro, F.; Vaccari, A. Hydrotalcite–type anionic clays: Preparation, properties and applications. *Catal. Today* **1992**, *11*, 173–301. [CrossRef]
22. Mills, S.J.; Christy, A.G.; Génin, J.M.R.; Kameda, T.; Colombo, F. Nomenclature of the hydrotalcite supergroup: natural layered double hydroxides. *Mineral. Mag.* **2012**, *76*, 1289–1336. [CrossRef]
23. Othman, M.R.; Helwani, Z.; Martunus, W.J.N. Synthetic hydrotalcites from different routes and their application as catalysts and gas adsorbents: a review. *Appl. Organometal Chem.* **2009**, *23*, 335–346. [CrossRef]
24. Jitianu, M.; Balasoiu, M.; Zaharescu, M.; Jitianu, A.; Ivanov, A. Comparative Study of Sol-Gel and Coprecipitated Ni-Al Hydrotalcites. *J. Sol.-Gel. Sci. Techn.* **2000**, *19*, 453–457. [CrossRef]
25. Qu, J.; Sha, L.; Wu, C.; Zhang, Q. Applications of Mechanochemically Prepared Layered Double Hydroxides as Adsorbents and Catalysts: A Mini-Review. *Nanomaterials* **2019**, *9*, 80. [CrossRef]
26. Miyata, S. Physico-chemical properties of synthetic hydrotalcites in relation to composition. *Clays. Clay. Miner.* **1980**, *28*, 50–56. [CrossRef]
27. Roelofs, J.C.A.A.; Bokhoven, J.A.; Dillen, A.J.; Geus, J.W.; Jong, K.P. The Thermal Decomposition of Mg±Al Hydrotalcites: Effects of Interlayer Anions and Characteristics of the Final Structure. *Chem. Eur. J.* **2002**, *8*, 5571–5579. [CrossRef]
28. Iqbal, M.A.; Fedel, M. Effect of Synthesis Conditions on the Controlled Growth of MgAl–LDH Corrosion Resistance Film: Structure and Corrosion Resistance Properties. *Coatings* **2019**, *9*, 30. [CrossRef]
29. Yan, A.L.; Wang, X.C.; Cheng, J.P. Research Progress of NiMn Layered Double Hydroxides for Supercapacitors: A Review. *Nanomaterials* **2018**, *8*, 747. [CrossRef]
30. Coral, N.; Brasil, H.; Rodrigues, E.; Costa, C.E.F.; Rumjanek, V. Microwave-modified hydrotalcites for the transesterification of soybean oil. *Sust. Chem. Pharm.* **2019**, *11*, 49–53. [CrossRef]
31. Hájek, M.; Tomášová, A.; Kocík, J.; Podzemná, V. Statistical evaluation of the mutual relations of properties of Mg/Fe hydrotalcites and mixed oxides as transesterification catalysts. *Appl. Clay. Sci.* **2018**, *154*, 28–35. [CrossRef]
32. Fatimah, I.; Rubiyanto, D.; Nugraha, J. Preparation, characterization, and modelling activity of potassium fluoride modified hydrotalcite for microwave assisted biodiesel conversion. *Sust. Chem. Pharm.* **2018**, *8*, 63–70. [CrossRef]
33. Tajuddin, N.A.; Manayil, J.C.; Isaacs, M.A.; Parlett, C.M.A.; Lee, A.F.; Wilson, K. Alkali-Free Zn–Al Layered Double Hydroxide Catalysts for Triglyceride Transesterification. *Catalysts* **2018**, *8*, 667. [CrossRef]
34. Navajas, A.; Campo, I.; Moral, A.; Echave, J.; Sanz, O.; Montes, M.; Odriozola, J.A.; Arzamendi, G.; Gandía, L.M. Outstanding performance of rehydrated Mg-Al hydrotalcites as heterogeneous methanolysis catalysts for the synthesis of biodiesel. *Fuel* **2018**, *211*, 173–181. [CrossRef]
35. Dhawan, M.S.; Yadav, G.D. Insight into a catalytic process for simultaneous production of biodiesel and glycerol carbonate from triglycerides. *Catal. Today* **2018**, *309*, 161–171. [CrossRef]
36. Wang, Y.T.; Fang, Z.; Zhang, F.; Xue, B.J. One-step production of biodiesel from oils with high acid value by activated Mg–Al hydrotalcite nanoparticles. *Bioresour. Technol.* **2015**, *193*, 84–89. [CrossRef] [PubMed]
37. Prado, R.G.; Almeida, G.D.; Carvalho, M.M.O.; Galvao, L.M.; Bejan, C.C.C.; Costa, L.M.; Pinto, F.G.; Tronto, J.; Pasa, V.M.D. Multivariate Method for Transesterification Reaction of Soybean Oil Using Calcined Mg–Al Layered Double Hydroxide as Catalyst. *Catal. Lett.* **2014**, *144*, 1062–1073. [CrossRef]
38. Macala, G.S.; Robertson, A.W.; Johnson, C.L.; Day, Z.B.; Lewis, R.S.; White, M.G.; Iretskii, A.V.; Ford, P.C. Transesterification Catalysts from Iron Doped Hydrotalcite-like Precursors: Solid Bases for Biodiesel Production. *Catal. Lett.* **2008**, *122*, 205–209. [CrossRef]

39. Li, E.; Ping Xu, Z.; Rudolph, V. MgCoAl–LDH derived heterogeneous catalysts for the ethanol transesterification of canola oil to biodiesel. *Appl. Catal. B* **2009**, *88*, 42–49. [CrossRef]
40. Peña-Rodríguez, R.; Márquez-López, E.; Guerrero, A.; Chiñas, L.E. Hydrothermal synthesis of cobalt (II) 3D metal-organic framework acid catalyst applied in the transesterification process of vegetable oil. *Mater. Lett.* **2018**, *217*, 117–119. [CrossRef]
41. Jamilah; Krisnandia, Y.K.; Sihombing, R. Synthesis and characterization of mesoporous Co/ZSM5 catalyst and activity study on transesterification reaction. *AIP Conf. Proc.* **2016**, *1729*, 020042. [CrossRef]
42. Nuithitikul, K.; Prasitturattanachai, W.; Hasinc, W. Comparison in catalytics activities of sulfated Cobalt-Tin and sulfated aluminum-Tin mixed oxiddes for esterification of free fatty acis to produce methyl esteres. *Energy Procedia* **2017**, *138*, 75–80. [CrossRef]
43. Nasrollahzadeh, M.; Bagherzadeh, M.; Karimi, H. Preparation, characterization and catalytic activity of $CoFe_2O_4$ nanoparticles as a magnetically recoverable catalyst for selective oxidation of benzyl alcohol to benzaldehyde and reduction of organic dyes. *J. Colloid. Interface Sci.* **2016**, *465*, 271–278. [CrossRef] [PubMed]
44. Soares, J.M.; Conceição, O.L.A.; Machado, F.L.A.; Prakash, A.; Radha, S.; Nigam, A.K. Magnetic properties of the nanocomposite $CoFe_2O_4$/FeCo-FeO at a high H/T regime. *J. Magn. Magn. Mater.* **2015**, *374*, 192–196. [CrossRef]
45. Knothe, G.; Steidley, K.R. Kinematic viscosity of biodiesel fuel components and related compounds. Influence of compound structure and comparison to petrodiesel fuel components. *Fuel* **2005**, *84*, 1059–1065. [CrossRef]
46. Kollar, S.R.M.; Novotny, E.H.; Nascimento, C.J.; Suarez, P.A.Z. Nuclear Magnetic Resonance (1.40 T) and Mid Infrared (FTIR-ATR) Associated with Chemometrics as Analytical Methods for the Analysis of Methyl Ester Yield Obtained by Esterification Reaction. *J. Braz. Chem. Soc.* **2017**, *28*, 1917–1925. [CrossRef]
47. Olutoye, M.A.; Hameed, B.H. ScienceDirectKinetics and deactivation of a dual-site heterogeneous oxide catalystduring the transesterification of crude jatropha oil with methanol. *J. Taibah. Univ. Sci.* **2016**, *10*, 685–699. [CrossRef]
48. World Intellectual Property Organization. Patent Scope. Available online: https://patentscope.wipo.int/search/es/detail.jsf?docId=MX194961824&redirectedID=true (accessed on 31 January 2019).